ACADEMIC PRESS

Available online at www.sciencedirect.com
SCIENCE DIRECT®

Journal of Solid State Chemistry 174 (2003) 35–43

JOURNAL OF SOLID STATE CHEMISTRY

http://elsevier.com/locate/jssc

X-ray and neutron powder diffraction study of the order–disorder transition in Eu_2IrH_5 and the mixed crystal compounds $Eu_{2-x}A_xIrH_5$ (A = Ca, Sr; x = 1.0, 1.5)

H. Kohlmann,[a,b,*] R.O. Moyer Jr.,[c] T. Hansen,[d] and K. Yvon[a]

[a] *Laboratoire de Cristallographie, Université de Genève, Quai E. Ansermet 24, 1211 Genève 4, Switzerland*
[b] *FR 8.14 Anorganische und Analytische Chemie und Radiochemie, Universität des Saarlandes, Postfach 15 11 50, 66041 Saarbrücken, Germany*
[c] *Department of Chemistry, Trinity College, Hartford, CT 06106-3100, USA*
[d] *Institut Laue-Langevin, Avenue des Martyrs, BP 156, 38042 Grenoble Cedex, France*

Received 14 November 2002; received in revised form 6 March 2003; accepted 15 March 2003

Abstract

The title compounds and their deuterides have been prepared by solid-state and solid–gas reactions from the elements and investigated by X-ray and neutron powder diffraction as a function of temperature. At room temperature they crystallize with an anion-deficient cubic K_2PtCl_6-type structure (space group $Fm\bar{3}m$) in which five hydrogen (deuterium) atoms surround iridium randomly on six octahedral sites with average bond distances of Ir–D = 169–171 pm. At low temperature they undergo a tetragonal deformation (space group $I4/mmm$) to the partially ordered Sr_2IrD_5 ($T = 4.2$ K)-type structure in which four hydrogen (deuterium) atoms occupy planar sites with full occupancy (Ir–D = 166–170 pm) and two hydrogen (deuterium) atoms axial sites (Ir–D = 174–181 pm) with ~50% occupancy, i.e., the data are consistent with a mixture of square–pyramidal $[IrD_5]^{4-}$ complexes pointing in two opposite directions. The transitions occur at ~240 K ($Eu_{0.5}Ca_{1.5}IrD_5$, $Eu_{0.5}Sr_{1.5}IrD_5$), ~210 K ($EuSrIrD_5$), ~200 K ($EuCaIrD_5$, Eu_2IrD_5), and are presumably of first order.

Keywords: Complex metal hydrides; Metal–hydrogen complexes; Iridium–hydride complexes; Order–disorder transition; Neutron powder diffraction

1. Introduction

Iridium-based compounds of composition A_2IrH_5 (A = alkali-earth or divalent rare-earth element) belong to the class of the so-called "complex transition metal hydrides" (for a recent review see Ref. [1]). At room temperature they crystallize with a hydrogen-deficient cubic K_2PtCl_6-type structure (space group $Fm\bar{3}m$) in which five hydrogen (deuterium) atoms surround iridium randomly on six octahedral sites. At low temperature some members undergo a tetragonal deformation to a partially ordered structure such as Sr_2IrD_5 (space group $I4/mmm$) [2,3], while others appear not to transform such as Eu_2IrD_5 for which no transition has been observed down to $T = 4$ K [4]. Given the close structural similarity between europium- and strontium-based hydrides [5,6] and in view of recent progress in the structure determination by neutrons of heavy absorbing europium hydrides [5–9], it seemed worthwhile to reinvestigate Eu_2IrD_5 and to study further members of the previously reported solid solution series $Eu_{2-x}Ca_xIrD_5$ and $Eu_{2-x}Sr_xIrD_5$ [10].

2. Experimental details

2.1. Synthesis

Freshly prepared samples of composition $Eu_{2-x}A_xIrD_5/H_5$ (A = Ca, Sr; x = 0.0, 1.0, 1.5) were obtained following the procedures described earlier [10,11]. All metal constituents consisted of natural isotope mixtures (Ir: Electronic Space Products International, Inc.; Ca: K&K Laboratories; Eu, Sr: A.D. Mackay, Inc.). Care was exercised in order to reduce sources of oxygen contamination in the formation of these hydrides. Even though the purity level as advertised by the vendor was

*Corresponding author. Fax: +1-681-302-4233.
E-mail address: h.kohlmann@mx.uni-saarland.de (H. Kohlmann).

0022-4596/03/$ - see front matter © 2003 Elsevier Science (USA). All rights reserved.
doi:10.1016/S0022-4596(03)00171-3

3 N, it was essential to vacuum distill the calcium, strontium, and europium metals at 1.3 mPa and 1073 K. The purified metal was deposited onto a cold finger and the metal oxide contaminant remained in the distilling cup and was discarded. The 3 N purity iridium metal powder was oxide free and used as received. All of the metal and metal hydride handling was done in an atmosphere of argon. The 3 N pure hydrogen was passed through a heated palladium tube filter prior to any hydriding. CP grade (99.5% pure) deuterium was purchased from Matheson Gas Products and used without any further purification.

Binary metal hydrides were formed by first placing small chips (~3–4 mm in length) of calcium, strontium, or europium in a molybdenum boat. The boat was inserted into a quartz reaction tube and the tube was then attached to an all glass vacuum line. The system was evacuated to 1.3 mPa after which either deuterium or hydrogen was introduced to approximately 10 kPa. The binary metal hydride was formed by heating the metal to approximately 670–770 K in approximately 10 kPa of gas. The metal hydride was removed from the apparatus and the quartz tube was transferred to the glove bag. The product was subsequently crushed by rapidly gyrating the sample in a small (~2 mL) agate ball mill. The powders were then mixed with iridium metal powder (−325 mesh) in the appropriate mole ratios and the homogeneous mass was compressed at 550 MPa. The resultant pellet was placed in a molybdenum boat that was inserted into a quartz reaction tube. The tube was attached to a glass vacuum line and evacuated. Hydrogen (deuterium) was introduced to approximately 10 kPa and the sample heated to 973 K. After completion of the hydrogenation reaction the products were removed from the furnace and crushed easily into a powder for subsequent structural analyses. The mixed crystal metal hydride formation is described according to the following equation:

$$(2-x)\mathrm{EuH_2(s)} + (x)A\mathrm{H_2(s)} + \mathrm{Ir(s)} + 1/2\mathrm{H_2/D_2(g)} \rightarrow \mathrm{Eu_{2-x}}A_x\mathrm{IrH_5/D_5(s)} \quad (A = \mathrm{Ca, Sr};\ x = 0.0,\ 1.0,\ 1.5).$$

2.2. X-ray powder diffraction

X-ray powder diffraction data for Eu_2IrH_5, $Eu_{0.5}Ca_{1.5}IrD_5$, $EuCaIrD_5$, $EuSrIrD_5$, and $Eu_{0.5}Sr_{1.5}IrD_5$ were taken in the temperature interval 7–298 K on a Guinier powder diffractometer equipped with a closed cycle He cryostat (Huber G645, Cu$K\alpha_1$ radiation, $18° \leqslant 2\theta \leqslant 100°$, $\Delta 2\theta = 0.02°$, 20 s data collection time per step, sample enclosed between two PET foils, internal standard silicon). The room temperature data confirmed the cubic K_2PtCl_6-type metal atom arrangement, whereas the low temperature data showed a splitting of Bragg reflections indicative for the occurrence of a cubic-to-tetragonal phase transition. Some of these reflections are marked in Fig. 1 for $EuCaIrD_5$. Structure refinements were carried out with the program DBWS-9411 [12]. The 2θ scale was calibrated by fitting a second-order polynomial against the reflections of the internal standard silicon. For the Rietveld refinements scale factors, lattice parameters, overall Debye–Waller factors and peak shape parameters (pseudo-Voigt function) were refined. Iridium was detected as a minority phase in all samples, whereas EuO was detected only in $Eu_{0.5}Sr_{1.5}IrD_5$ and Eu_2IrH_5. The contribution of hydrogen (deuterium) to the patterns was neglected. The atomic displacement and peak shape parameters of the minority phases were constrained to be equal to those of the main deuteride phase. Residuals were in the ranges $9\% < R_p < 12\%$, $12\% < R_{wp} < 15\%$, $1.3 < S < 1.6$. Lattice parameters at room and low (7–10 K) temperature are listed in Table 1. Fig. 2a–d shows the temperature dependence of the lattice parameters of: (a) $EuSrIrD_5$, (b) $Eu_{0.5}Sr_{1.5}IrD_5$, (c) $EuCaIrD_5$, and (d) $Eu_{0.5}Ca_{1.5}IrD_5$.

2.3. Neutron powder diffraction

In order to reduce effects due to neutron absorption by europium the samples (1.5 g $Eu_{0.5}Ca_{1.5}IrD_5$, 1.2 g

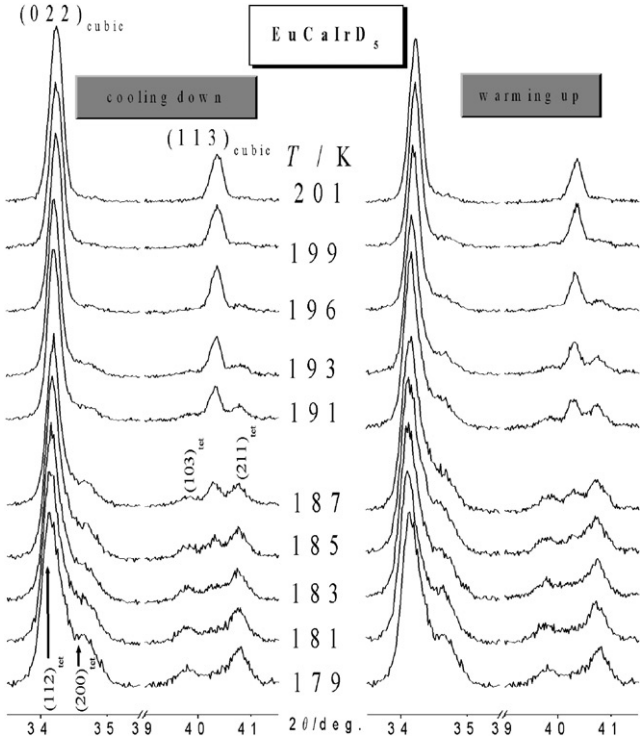

Fig. 1. The phase transition in $EuCaIrD_5$ as studied by temperature-dependent X-ray powder diffraction. The splitting of two peaks, $(022)_{cubic}$ and $(113)_{cubic}$, of the cubic phase into $(112)_{tet}/(200)_{tet}$ and $(103)_{tet}/(211)_{tet}$ of the tetragonal phase is shown on cooling down (left) and warming up (right).

Table 1
Lattice parameters of Eu_2IrH_5 and $Eu_{2-x}A_xIrD_5$ (A = Sr, Ca; x = 1.0, 1.5) as derived from Rietveld refinement on X-ray powder diffraction data

	Cubic K_2PtCl_6 type, $Fm\bar{3}m$	Tetragonal Sr_2IrD_5 (T = 4 K) type, $I4/mmm$
Eu_2IrH_5	$a(T = 298\,K) = 758.24(4)$ pm	$a(T = 7\,K) = 527.59(6)$ pm $c(T = 7\,K) = 775.4(1)$ pm
$EuSrIrD_5$	$a(T = 293\,K) = 760.55(3)$ pm	$a(T = 7\,K) = 528.78(7)$ pm $c(T = 7\,K) = 776.33(18)$ pm
$Eu_{0.5}Sr_{1.5}IrD_5$	$a(T = 298\,K) = 762.10(2)$ pm	$a(T = 10\,K) = 530.15(3)$ pm $c(T = 10\,K) = 778.32(6)$ pm
$EuCaIrD_5$	$a(T = 296\,K) = 741.75(2)$ pm	$a(T = 8\,K) = 515.80(4)$ pm $c(T = 8\,K) = 757.49(11)$ pm
$Eu_{0.5}Ca_{1.5}IrD5$	$a(T = 298\,K) = 733.42(2)$ pm	$a(T = 10\,K) = 509.54(3)$ pm $c(T = 10\,K) = 751.36(7)$ pm

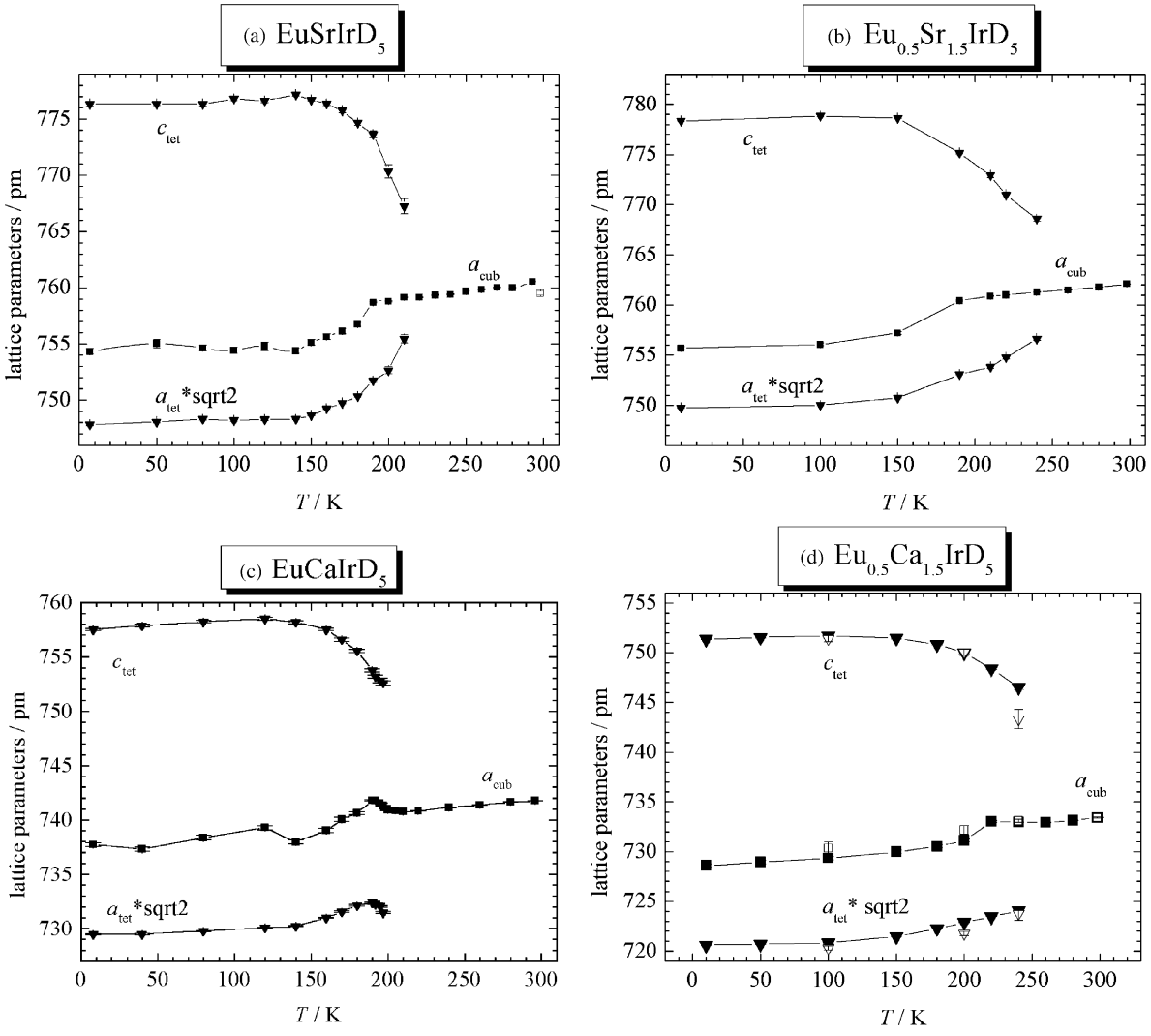

Fig. 2. Phase transition in: (a) $EuSrIrD_5$, (b) $Eu_{0.5}Sr_{1.5}IrD_5$, (c) $EuCaIrD_5$, and (d) $Eu_{0.5}Ca_{1.5}IrD_5$ studied by temperature-dependent X-ray (filled symbols) and neutron powder diffraction (open symbols). The error bars correspond to $\pm\sigma$ of the lattice parameters as refined by the Rietveld method.

$EuSrIrD_5$, and 3.0 g Eu_2IrD_5) were filled in double-walled vanadium cans (64 mm length, 9.15 mm inner diameter of the outer cylinder, 0.6 mm annular thickness, hermetically closed by an indium wire) and neutron wavelengths close to the minimum of the neutron absorption cross-section of natural europium were chosen [8,13]. Except for Eu_2IrD_5 all data were collected on the powder diffractometer D4b (ILL, Grenoble, France) as equipped with two 64-cell ^3He multi-detectors covering 6.4° and 12.8° in 2θ, respectively. Due to a failure of the hot source it was operating only at ~30% of its original neutron flux. Wavelengths and zero shifts were determined to 70.647(8) pm and −0.1713(2)°, respectively, by measuring a standard nickel sample. For $Eu_{0.5}Ca_{1.5}IrD_5$ and $EuSrIrD_5$ data were collected as a function of temperature with a step size of 1.9° and a resolution of 0.1° during 3.75 h. For $Eu_{0.5}Ca_{1.5}IrD_5$ four data sets were recorded at $T = 298$, 240, 200, and 100 K and at intervals of ~1–1.5 h between each measurement. Due to technical problems with the temperature control the $EuSrIrD_5$ sample had to be mounted in the cold cryostat at 123 K. During the 3.5 h scan the temperature dropped inadvertently from 123 to 116 K. The sample was then cooled to a constant temperature of 1.6 K and diffraction data were collected at this temperature over a period of 7 h. At this point the cryostat was disengaged from the sample, the sample was warmed to room temperature, and diffraction data were then collected once again over a period of 3.5 h. For Eu_2IrD_5 data were taken on D20 (ILL, Grenoble, France) equipped with a large-area linear curved position-sensitive detector, at constant temperatures of 298 K (1.1 h), 100 K (3.4 h), and 2 K (3.4 h) with cooling rates of 100 K/h between data collections. Wavelength and zero shift were determined to 79.923(8) pm and 0.776(5)°, respectively, from a measurement of a standard silicon sample.

2.4. Structure refinements

Crystal structures were refined with the Rietveld method (computer program FullProf [14]) by using pseudo-Voigt functions for reflection profiles. The background was modelled by linear interpolation between 15 and 30 points. The neutron wavelengths and zero points of the diffractometers were fixed at the experimentally determined values (see above), and secondary phases (EuO, Ir) and vanadium (sample holder) were included in the refinements. The reflection profiles and half-width parameters were constrained to be equal to those of the main phase. For reasons outlined before [15] the data were not corrected for absorption effects ($\mu = 6.1$, and $9.5\,cm^{-1}$ at $\lambda = 70.647$ pm for $Eu_{0.5}Ca_{1.5}IrD_5$ and $EuSrIrD_5$, respectively, and $\mu = 18.7\,cm^{-1}$ for Eu_2IrD_5 at $\lambda = 79.923$ pm). All phases were found to crystallize with an anion-deficient cubic K_2PtCl_6-type structure (space group $Fm\bar{3}m$) having deuterium site occupancies of ~5/6. For the mixed crystals the assumption of random occupancy of A sites was confirmed. On lowering the temperature a splitting of reflections and the occurrence of new reflections indicated the onset of a structural phase transition. Reflection conditions were consistent with space group $I4/mmm$. No reflections (hkl) with $h + k + l \neq 2n$ were observed that would indicate a further lowering of symmetry. The

Table 2
Crystal structure data of cubic Eu_2IrD_5 ($T = 298$ K), $EuSrIrD_5$ ($T = 298$ K), and $Eu_{0.5}Ca_{1.5}IrD_5$ ($T = 298$ and 240 K) refined from neutron powder diffraction data

Space group $Fm\bar{3}m$ (no. 225)					
Atom	Site	Symmetry	x/a	y/b	z/c
A	8*c*	−43*m*	1/4	1/4	1/4
Ir	4*a*	$m\bar{3}m$	0	0	0
D	24*e*	4*m.m*	x	0	0
Compound	Eu_2IrD_5	$EuSrIrD_5$	$Eu_{0.5}Ca_{1.5}IrD_5$		
T/K	298	298	298	240	
a/pm	756.7(2)	759.5(2)	733.41(7)	733.1(2)	
A	Eu	1/2Eu + 1/2Sr	1/4Eu + 3/4Ca		
$B_{iso}(A)/10^4\,pm^2$	1.1(2)	2.3(2)	1.1(1)	1.1(2)	
$B_{iso}(Ir)/10^4\,pm^2$	0.8(2)	2.2(2)	0.68(7)	0.6(1)	
x(D)	0.223(1)	0.225(1)	0.2309(5)	0.2300(9)	
$B_{iso}(D)/10^4\,pm^2$	2.0(1)	3.0(2)	1.75(9)	1.5(2)	
Occupation (D)	0.855(27)	0.882(22)	0.833(11)	0.808(16)	
Refined composition	$Eu_2IrD_{5.13(16)}$	$EuSrIrD_{5.29(13)}$	$Eu_{0.5}Ca_{1.5}IrD_{5.00(7)}$	$Eu_{0.5}Ca_{1.5}IrD_{4.85(10)}$	
R_p	0.021	0.014	0.014	0.013	
R_{wp}	0.026	0.017	0.016	0.016	
R_{Bragg}	0.108	0.100	0.070	0.074	
S	1.23	1.71	2.33	2.23	

Table 3
Crystal structure data of tetragonal Eu_2IrD_5 ($T = 100$ K), $EuSrIrD_5$ ($T = 120$ K), and $Eu_{0.5}Ca_{1.5}IrD_5$ ($T = 100$ and 200 K) refined from neutron powder diffraction data

Space group $I4/mmm$ (no. 139)					
Atom	Site	Symmetry	x/a	y/b	z/c
A	4*d*	$\bar{4}m2$	0	1/2	1/4
Ir	2*a*	$4/mmm$	0	0	0
D1	8*h*	$m.2m$	x	x	0
D2	4*e*	$4mm$	0	0	z
Compound	Eu_2IrD_5	$EuSrIrD_5$	$Eu_{0.5}Ca_{1.5}IrD_5$		
T/K	100	120	100	200	
a/pm	527.0(1)	529.11	509.3(2)	510.4(1)	
c/pm	773.0(4)	776.61	751.4(3)	750.0(3)	
A	Eu	1/2Eu + 1/2Sr	1/4Eu + 3/4Ca		
B_{iso}(A)/10^4 pm^2	0.6(2)	3.0(5)	1.2(2)	1.1(2)	
B_{iso}(Ir)/10^4 pm^2	0.6(2)	0.1(1)	1.1(1)	1.1(1)	
x(D1)	0.228(1)	0.222(3)	0.2339(8)	0.2317(7)	
z(D2)	0.226(4)	0.259(6)	0.241(3)	0.239(2)	
B_{iso}(D1)/10^4 pm^2	1.2(2)	2.3(4)	1.8(2)	2.1(2)	
B_{iso}(D2)/10^4 pm^2	2.0(9)	5(1)	1.0(6)	1.2(6)	
Occupation (D2)	0.546(42)	0.78(9)	0.512(24)	0.528(16)	
Refined composition	$Eu_2IrD_{5.09(8)}$	$EuSrIrD_{5.5(2)}$	$Eu_{0.5}Ca_{1.5}IrD_{5.02(5)}$	$Eu_{0.5}Ca_{1.5}IrD_{5.06(3)}$	
R_p	0.010	0.016	0.014	0.013	
R_{wp}	0.012	0.019	0.018	0.016	
R_{Bragg}	0.083	0.170	0.086	0.062	
S	1.87	2.47	2.42	2.13	

low-temperature structures were described with the partially ordered tetragonal Sr_2IrD_5-type structure [2]. The refined occupancies of the deuterium sites led to a value not significantly different from 1.0 for D1 and to values close to 0.5 for D2. In all cases the phase transition was not complete and some cubic phase remained down to the lowest investigated temperatures. Due to the poor quality of the 120 K data of $EuSrIrD_5$ its lattice parameter had to be held constant at the value determined before from X-ray diffraction. Refinement results are listed in Tables. 2 and 3 and interatomic distances can be found in Table. 4. Graphical representations of the Rietveld refinements on the neutron data are shown in Figs. 3–5.

Table 4
Selected interatomic distances in Eu_2IrD_5, $Eu_{0.5}Ca_{1.5}IrD_5$, and $EuSrIrD_5$ in pm

	Eu_2IrD_5	$EuSrIrD_5$	$Eu_{0.5}Ca_{1.5}IrD_5$
A	Eu	1/2Eu + 1/2Sr	1/4Eu + 3/4Ca
Cubic: T/K	298	298	298
A–12D[a]	268.3(6)	269.2(5)	259.7(3)
Ir–6D[a]	168.8(9)	171.2(7)	169.4(4)
Closest D–D[a]	238.7(9)	242.1(7)	239.5(4)
Tetragonal : T/K	100	120	100
A–8D1	269.0(5)	270.4(9)	260.3(3)
A–4D2[b]	264.2(2)	264.7(1)	254.9(1)
Ir–4D1	169.9(9)	166(1)	168.6(4)
Ir–2D2[b]	174(3)	201(4)	181(2)
Closest D–D (D1–D1)	240.2(9)	235(2)	238.4(6)

[a] occupancy ~5/6, see Table 2.
[b] occupancy ~1/2, see Table 3.

3. Results and discussion

3.1. Cubic room temperature modification

At room temperature all members of the series $Eu_{2-x}A_xIrH(D)_5$ (A = Ca, Sr; $x = 0.0$, 1.0, 1.5) crystallize with an anion-deficient disordered K_2PtCl_6-type structure. As shown for Eu_2IrD_5 in Fig. 6 iridium is surrounded by an average of ~5 hydrogen (deuterium) atoms that are randomly distributed on octahedral sites. The refined deuterium contents for the various members do not differ significantly from the molar ratio of D/Ir = 5.0. In the mixed crystals the cations A (Eu^{2+}, Ca^{2+}, Sr^{2+}) are randomly distributed, in agreement with a previous study [10]. As expected from the ionic radii [16], the cubic cell parameter decreases considerably on replacement of europium by calcium, whereas it increases slightly on replacement by strontium (Table 1). The average iridium–deuterium distances are fairly constant throughout the series (169–171 pm, Table 4) which is accomplished by adjusting the free positional parameter x

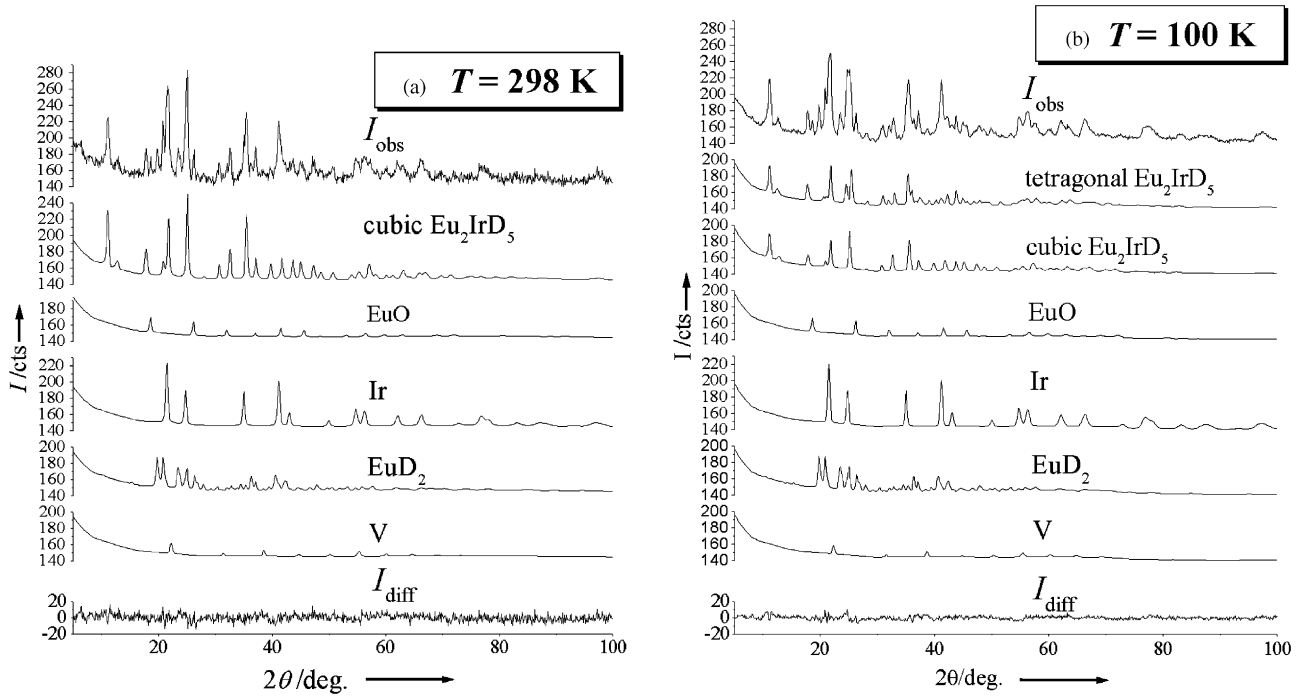

Fig. 3. Observed (top), calculated (middle) and difference (observed—calculated, bottom) neutron powder diffraction patterns of Eu_2IrD_5 at (a) $T = 298$ K and (b) $T = 100$ K (D20, $\lambda = 79.923(8)$ pm). All calculated patterns include the background. Intensity in total detector counts.

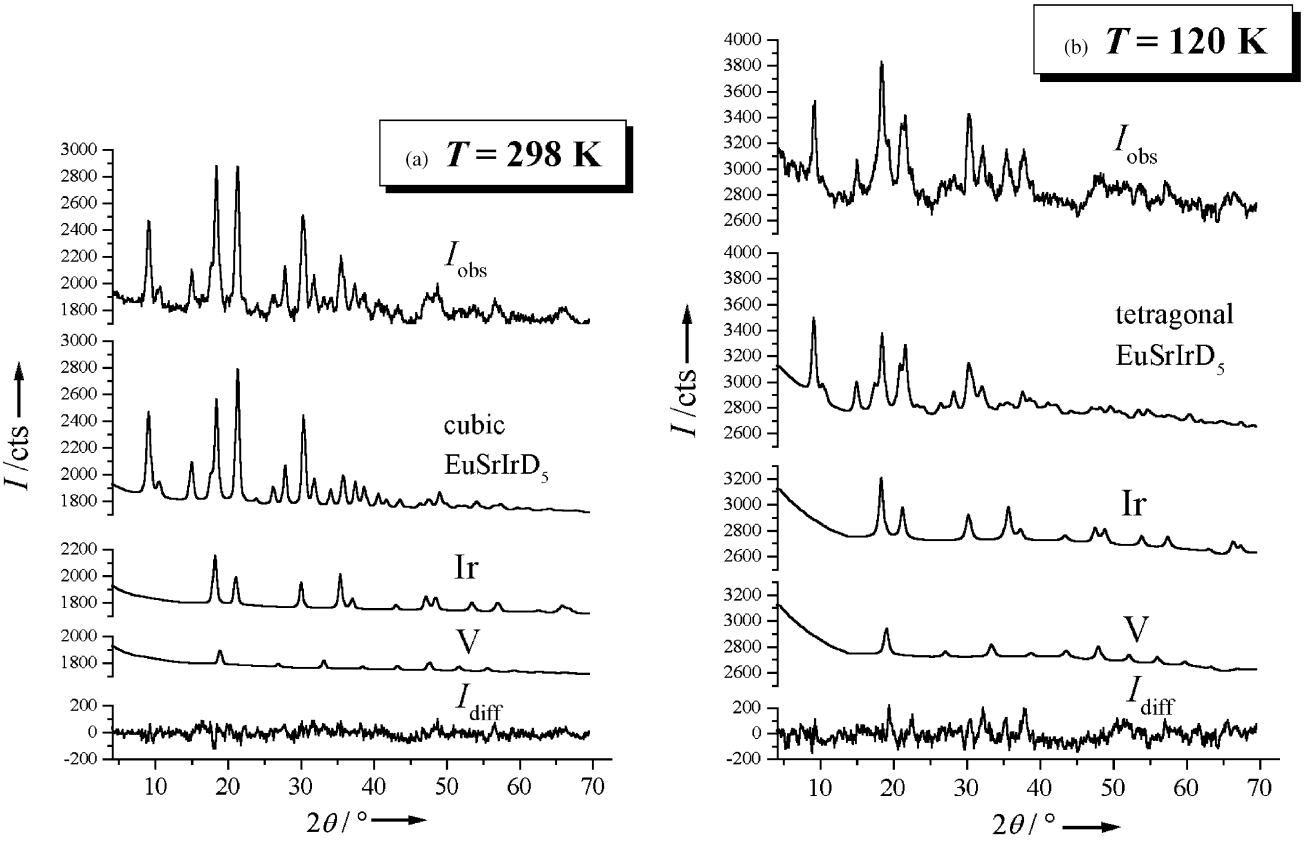

Fig. 4. Observed (top), calculated (middle) and difference (observed—calculated, bottom) neutron powder diffraction patterns of $EuSrIrD_5$ at (a) $T = 298$ K and (b) $T = 120$ K (D4b, $\lambda = 70.647(8)$ pm). All calculated patterns include the background. Intensity in total detector counts.

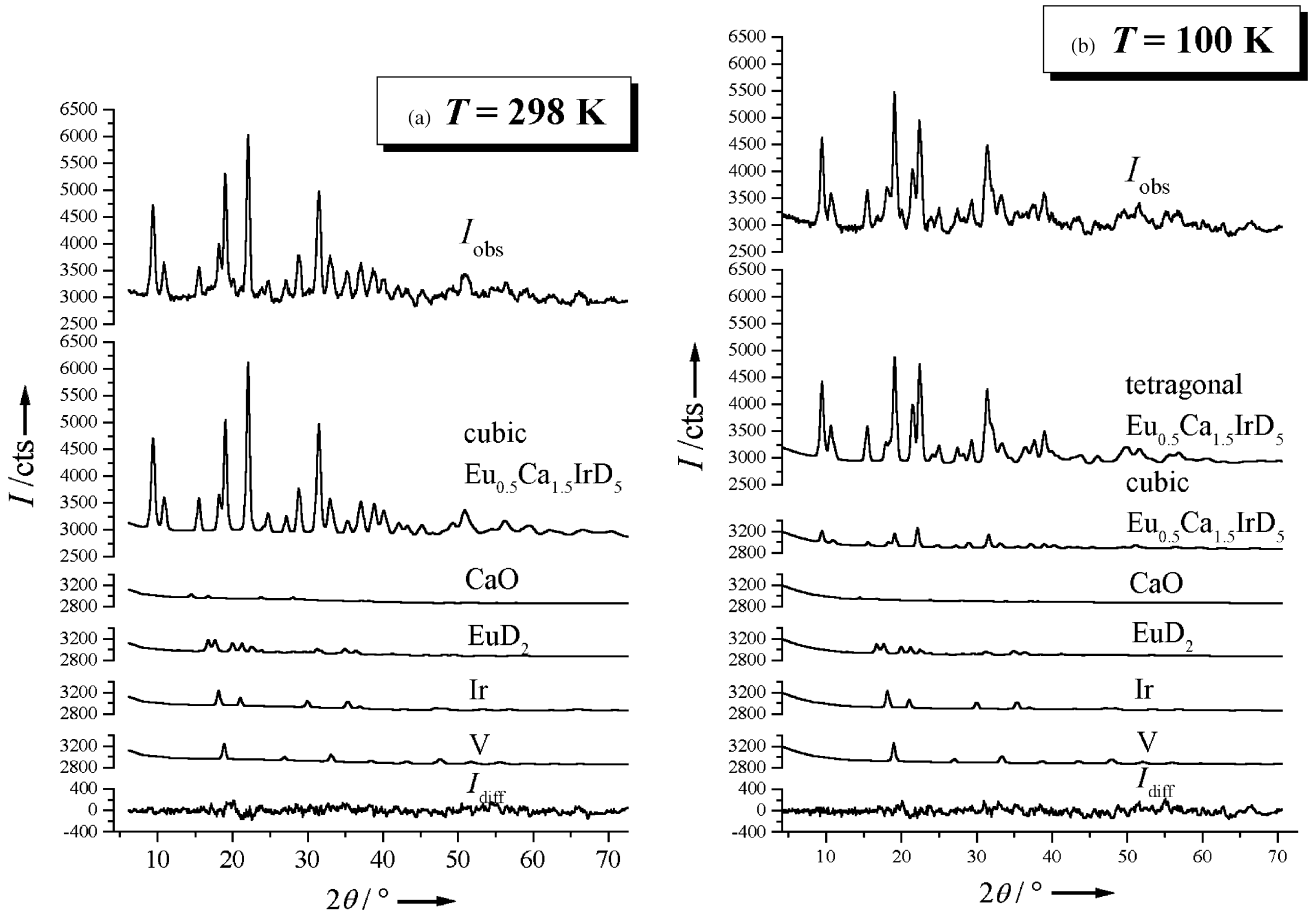

Fig. 5. Observed (top), calculated (middle) and difference (observed—calculated, bottom) neutron powder diffraction patterns of $Eu_{0.5}Ca_{1.5}IrD_5$ at (a) $T = 298$ K and (b) $T = 100$ K (D4b, $\lambda = 70.647(8)$ pm). All calculated patterns include the background. Intensity in total detector counts.

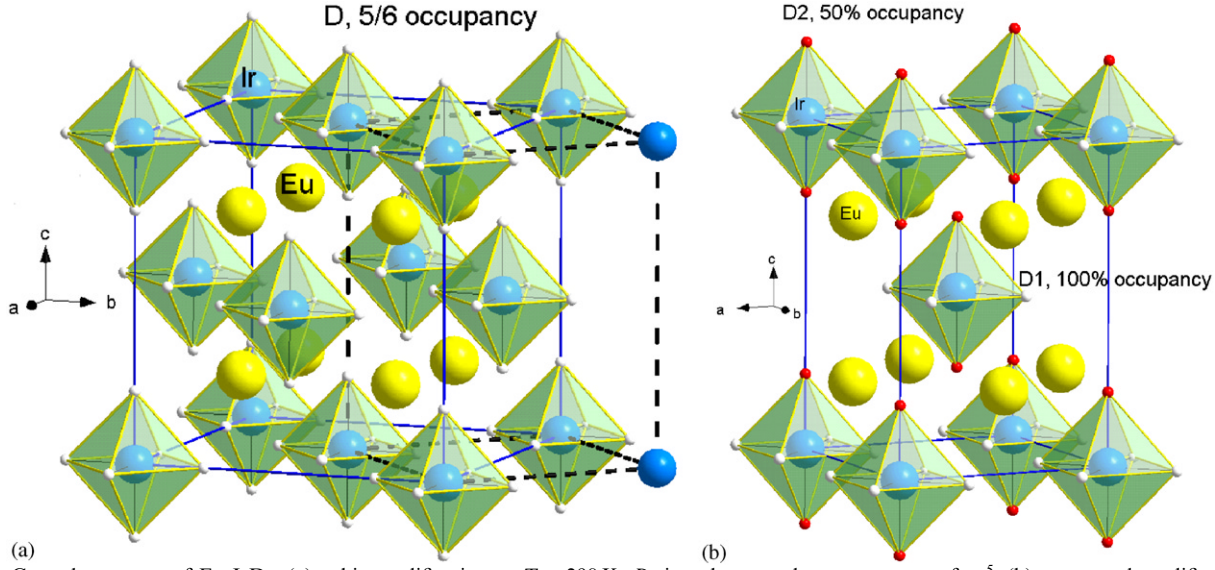

Fig. 6. Crystal structure of Eu_2IrD_5. (a) cubic modification at $T = 298$ K, D sites show random occupancy of $\approx\frac{5}{6}$; (b) tetragonal modification at $T = 100$ K, planar D sites fully occupied, apical D sites half occupied. The broken line in (a) shows the relation to the tetragonal unit cell in (b).

of deuterium on the 24*e* position (*x*00) according to the varying lattice parameter (Table 2). The average cation (*A*)–deuterium distances, on the other hand, vary with the lattice parameter, i.e., they are considerably shorter for calcium containing samples (260 pm in $Eu_{0.5}Ca_{1.5}IrD_5$) than for strontium containing samples (268 pm in Eu_2IrD_5

and 269 pm in $EuSrIrD_5$, see Table 4). The D–D separations are all longer than the so-called "blocking distance" of 210 pm. For cubic $Eu_{0.5}Ca_{1.5}IrD_5$ no significant change in structural parameters occurs on cooling to 240 K (Table 2).

3.2. Tetragonal low-temperature modification

Upon cooling the members of the $Eu_{2-x}A_xIrH(D)_5$ series all transform to a tetragonal low-temperature modification having the cell parameter relationships $c_{tet} \approx a_{cub}$, $a_{tet} \approx a_{cub}/\sqrt{2}$. These findings contrast with earlier neutron diffraction studies on Eu_2IrD_5 for which no phase transition was found down to 4 K [4]. As shown in Fig. 1 the splitting of two typical diffraction peaks of cubic $EuCaIrD_5$, (022) and (113) is fully reversible on cooling and warming up and shows a hysteresis of about 2 K. The temperature-dependent cell parameters for the mixed crystals as shown in Fig. 2 suggest that the transitions start at 200–240 K, depending on the degree of substitution and the nature of the cations A, and proceed down to about 150 K with a concomitant increase in cell distortion. A quantitative phase analysis (data not shown) shows that the proportion of tetragonal phase increases as the temperature is lowered and that 8–13% of the samples remain cubic even after slow cooling and prolonged (4 days) exposure at the lowest investigated temperature (7 K). This provides evidence for the transitions to be of first order. Clearly, the transitions in the $Eu_{2-x}A_xIrH(D)_5$ series are due to an ordering of deuterium atoms. However, in contrast to the cobalt analogue Mg_2CoD_5 [17] in which the deuterium atoms become fully ordered and form square–pyramidal $[CoH_5]^{4-}$ complexes, they are only partially ordered as in Sr_2IrD_5 ($T = 4.2$ K). Among the six available sites only four show full occupancy ("planar sites" D1) and two ~50% occupancy ("axial sites" D2), i.e., square–pyramidal $[IrD_5]^{4-}$ complexes are presumably pointing in two opposite directions (Fig. 6b). As with Mg_2CoD_5 and Mg_2IrD_5 the transition metal–deuterium bond distances are longer for the axial (Ir−D = 174–181 pm) than the planar sites (Ir−D = 166–170 pm) and correlate with an increase of the parameter ratio of the pseudo-cubic cell ($c/a = 1.04$). The only ordered, although distorted square–pyramidal $[IrD_5]^{4-}$ complex known so far are that in $Mg_6Ir_2D_{11}$ [18].

3.3. Symmetry relationships

The structural relationship between the cubic and the tetragonal phase can be illustrated by the symmetry tree as shown in Fig. 7. The space groups are consistent with a *translationengleiche* transition of index 3 that splits the deuterium position of the cubic structure into two crystallographic non-equivalent positions in the tetragonal structure of which one is fully and the other half occupied. No indication exists for a further symmetry reduction by a *klassengleiche* transition of index 2 to space group $P4/nmm$ such as for Mg_2CoD_5. The space group relation between the high- and low-temperature modification of the $Eu_{2-x}A_xIrH(D)_5$ series are consistent with a second-order phase transition. However, the rather abrupt changes in cell parameters as a function of temperature (Fig. 2) together with the coexistence of cubic and tetragonal phase down to very low-temperature point rather towards a first-order transition. The role of oxygen impurities in these transitions cannot be excluded. Previous studies in other metal hydride systems have shown [19] that surface oxidation can lead to incomplete order–disorder transitions. It is possible that similar conditions prevailed in the present $Eu_{2-x}A_xIrH(D)_5$ samples. As can be seen on Figs. 3–5 the amount of retained cubic phase correlates with the oxygen content of the sample. The sample with the highest EuO content (Eu_2IrD_5) also shows the largest fraction of cubic phase at low temperature. The retention of about 13% of cubic phase was also observed in the phase transition of Sr_2IrD_5 [2]. On the other hand, small deviations from the hydrogen (deuterium) content may also play a role. However, the methodology used in the present work does not allow an analysis of the deuterium content to be made at a degree of accuracy sufficient to answer this question.

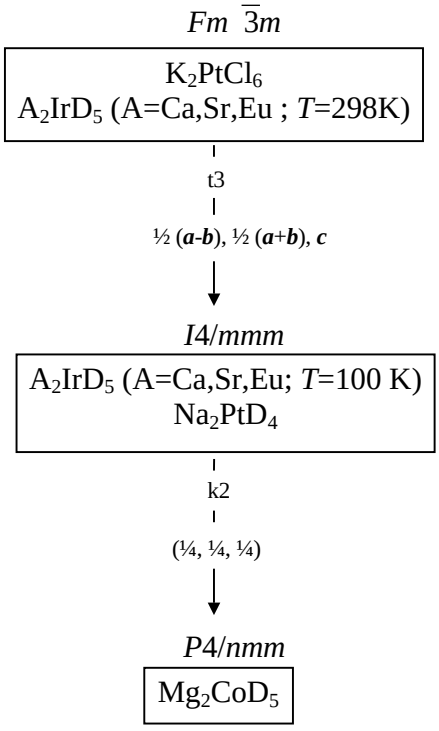

Fig. 7. *Bärnighausen* tree of the group–subgroup relationships between some cubic and tetragonal A_2MD_6, A_2MD_5, and A_2MD_4 compounds.

Acknowledgments

We gratefully acknowledge the help of Pierre Palleau and Dr. Gabriel Cuello (both ILL, Grenoble, France) with the neutron diffraction experiments on D4b. One of us (ROM) acknowledges a Trinity College Faculty Research Grant and thanks the University of Geneva for hospitality during a recent leave of absence. This work was supported by the Swiss National Science Foundation and the Swiss Federal Office of Energy.

References

[1] K. Yvon, Chimia 52 (1998) 613–619.
[2] J. Zhuang, J.M. Hastings, L.M. Corliss, R. Bau, C.Y. Wei, R.O. Moyer Jr., J. Solid State Chem. 40 (1981) 352–360.
[3] R.O. Moyer Jr., B. Toby, J. Alloys Compd. 2003, in press.
[4] J. Zhuang, W. Kunnmann, L.M. Corliss, J.M. Hastings, R.O. Moyer Jr., J. Solid State Chem. 48 (1983) 117–120.
[5] H. Kohlmann, H.E. Fischer, K. Yvon, Inorg. Chem. 40 (2001) 2608–2613.
[6] K. Yvon, H. Kohlmann, B. Bertheville, Chimia 55 (2001) 505–509.
[7] H. Kohlmann, F. Gingl, T. Hansen, K. Yvon, Angew. Chem. 111 (1999) 2145–2147;
H. Kohlmann, F. Gingl, T. Hansen, K. Yvon, Angew. Chem. Int. Ed. Engl. 38 (1999) 2029–2032.
[8] H. Kohlmann, Physica B 276–278 (2000) 288–289.
[9] H. Kohlmann, B. Bertheville, T. Hansen, K. Yvon, J. Alloys Compd. 322 (2001) 59–68.
[10] R.O. Moyer Jr., B.J. Burnim, R. Lindsay, J. Solid State Chem. 121 (1996) 56–60.
[11] R.O. Moyer Jr., R. Lindsay, D.F. Storey, Z. Phys. Chem., Neue Folge, 165 (1989) 83–94.
[12] R.A. Young, A. Sakthivel, T.S. Moss, C.O. Paive-Santos, J. Appl. Crystallogr. 28 (1995) 366–367.
[13] J.E. Lynn, J. Appl. Crystallogr. 22 (1989) 476–482.
[14] J. Rodriguez-Carvajal, FullProf.'98, 1998 (LLB, unpublished).
[15] H. Kohlmann, K. Yvon, J. Alloys Compd. 299 (2000) L16–L20.
[16] R.D. Shannon, Acta Crystallogr. Sect. A 32 (1976) 751–767.
[17] P. Zolliker, K. Yvon, P. Fischer, J. Schefer, Inorg. Chem. 24 (1985) 4177–4180.
[18] R. Cerny, J.-M. Joubert, H. Kohlmann, K. Yvon, J. Alloys Compd. 340 (2002) 180–188.
[19] I.I. Borisov, A.V. Irodova, O.A. Lavrova, G.V. Laskova, V.A. Somenkov, Sov. Phys. Solid State 26 (1984) 2031–2033.